

## A NOVEL IMAGE SEGMENTATION APPROACH BASED ON NEUTROSOPHIC SET AND IMPROVED FUZZY C-MEANS ALGORITHM

H. D. CHENG<sup>\*†‡</sup>, YANHUI GUO<sup>‡§</sup> and YINGTAO ZHANG<sup>\*¶</sup>

*\*School of Computer Science and Technology  
Harbin Institute of Technology  
Harbin, Heilongjiang, 150001, China*

*†Department of Computer Science, Utah State University  
Logan, UT 84322, USA*

*‡hd.cheng@aggiemail.usu.edu*

*‡http://cs.usu.edu/~cheng*

*§yanhui.guo@aggiemail.usu.edu*

*¶yingtao@hit.edu.cn*

Image segmentation is an important component in image processing, pattern recognition and computer vision. Many segmentation algorithms have been proposed. However, segmentation methods for both noisy and noise-free images have not been studied in much detail.

Neutrosophic set (NS), a part of neutrosophy theory, studies the origin, nature, and scope of neutralities, as well as their interaction with different ideational spectra. However, neutrosophic set needs to be specified and clarified from a technical point of view for a given application or field to demonstrate its usefulness.

In this paper, we apply neutrosophic set and define some operations. Neutrosophic set is integrated with an improved fuzzy *c*-means method and employed for image segmentation. A new operation,  $\alpha$ -mean operation, is proposed to reduce the set indeterminacy. An improved fuzzy *c*-means (IFCM) is proposed based on neutrosophic set. The computation of membership and the convergence criterion of clustering are redefined accordingly. We have conducted experiments on a variety of images. The experimental results demonstrate that the proposed approach can segment images accurately and effectively. Especially, it can segment the clean images and the images having different gray levels and complex objects, which is the most difficult task for image segmentation.

*Keywords:* Image segmentation; fuzzy clustering; neutrosophic set; indeterminacy.

### 1. Introduction

Image segmentation is a critical and essential process and is one of the most difficult tasks in computer vision, image processing and pattern recognition, which determines the quality of the final analysis and plays an important role in a variety of applications such as robot vision, object recognition, medical imaging, etc.

Segmentation separates objects from the background. Reference 1 considered image segmentation as a bridge between a low-level vision subsystem (such as noise

reduction, edge extraction), and a high-level vision subsystem (such as object recognition and scene interpretation).<sup>1</sup> After segmentation, the input image is mapped into a description of the regions with some features for high-level vision tasks.

Gray image segmentation approaches are based on either discontinuity and/or homogeneity. The approaches based on discontinuity tend to partition an image by detecting isolated points, lines and edges according to the abrupt changes of the gray levels. The approaches based on homogeneity include thresholding, clustering, region growing, and region splitting and merging.<sup>1</sup>

Image segmentation is a process dividing an image into different regions such that each region is, but the union of any two adjacent regions is not homogeneous; i.e. it is a partition of image  $I$  into non-overlapping regions  $S_i$ :<sup>1</sup>

$$\bigcup S_i = I \quad \text{and} \quad S_i \cap S_j = \phi, \quad i \neq j$$

Fuzzy theory has been applied to image segmentation, which retains more information than that of the hard segmentation methods.<sup>2,3</sup>

Fuzzy  $c$ -means (FCM)<sup>4,5</sup> is a fuzzy clustering method allowing a piece of data to belong to two or more clusters, which is frequently used in computer vision, pattern recognition and image processing. The fuzzy  $c$ -means algorithm obtains segmentation results by using fuzzy classification.<sup>6</sup>

For classical set, the indeterminacy of each element in the set could not be evaluated and described. Fuzzy set<sup>7</sup> has been applied to handle uncertainty. The traditional fuzzy set uses a real number  $\mu_A(x) \in [0, 1]$  to represent the membership of the set  $A$  defined on universe  $X$ . If  $\mu_A(x)$  itself is uncertain, it is hard to be defined by a crisp value.<sup>8</sup> In some applications such as expert system, belief system and information fusion, we should consider not only the truth membership, but also the falsity membership and the indeterminacy of the two memberships. It is hard for classical fuzzy set to solve such problems.<sup>8</sup>

Neutrosophy is a new branch of philosophy, and studies the origin, nature, and scope of neutralities.<sup>9</sup> It considers proposition, theory, event, concept, or entity,  $\langle A \rangle$  is in relation with its opposite  $\langle \text{Anti-}A \rangle$  and the neutrality  $\langle \text{Neut-}A \rangle$  which is neither  $\langle A \rangle$  nor  $\langle \text{Anti-}A \rangle$ . Neutrosophy is the basis of neutrosophic logic, neutrosophic probability, neutrosophic set, and neutrosophic statistics.<sup>9</sup>

Neutrosophy provides a powerful tool to deal with the indeterminacy. The indeterminacy is quantified and the memberships of three subsets ( $\langle A \rangle$ ,  $\langle \text{Anti-}A \rangle$  and  $\langle \text{Neut-}A \rangle$ ) are defined in different domains. For example, when reviewers are invited to review a paper, they need to rank the paper (using  $\mu$ ) and indicate how well (using  $W$ ) they understand the related field.<sup>10</sup> Assume that two reviewers A and B review a paper with  $\mu_A = \mu_B = 0.9$  and  $W_A = 0.9$  and  $W_B = 0.7$ . Then,  $\mu_A$  and  $\mu_B$  should have different effects on the decision of the paper. This kind of problems can be solved better by using neutrosophic set.

In neutrosophic set, a set  $A$  is described by three subsets:  $\langle A \rangle$ ,  $\langle \text{Neut-}A \rangle$  and  $\langle \text{Anti-}A \rangle$  are interpreted as truth, indeterminacy and falsity subsets. Reference 11

proposed a thresholding algorithm based on neutrosophic set,<sup>11</sup> which could select the thresholds for images, even noisy images, automatically and effectively. Reference 12 applied the neutrosophic set and defined some concepts and operators for image denoising.<sup>12</sup>

Reference 10 combined neutrosophic set with  $K$ -means clustering method for image segmentation.<sup>10</sup> The image is transformed into neutrosophic set ( $NS$ ) domain and described using three membership sets,  $T$ ,  $F$  and  $I$ . The entropy in  $NS$  domain is defined and employed to evaluate the indeterminacy. Two operations were proposed to reduce the set indeterminacy. The operations are performed iteratively until the entropy unchanged. Finally, the image was segmented using the  $K$ -means clustering method. The method could perform better on both the clean and noisy images. However, it would fail if the entropy is still changing, and it could cause edges and boundaries blur. Moreover,  $K$ -means cluster would perform poorly when some pixels did not completely belong to just one cluster, such as the edge pixels.

In order to overcome the drawback of the method,<sup>10</sup> we propose a novel image segmentation approach based on neutrosophic theory and a modified fuzzy  $c$ -means algorithm, the  $\alpha$ -fuzzy  $c$ -means algorithm. The image is transformed into  $NS$  domain and an  $\alpha$ -mean operation is proposed and employed iteratively to reduce the indeterminacy of the image. In  $\alpha$ -fuzzy  $c$ -means clustering method, the membership value is redefined and updated according to the indeterminacy value. Finally, the iterative process is terminated and the image is segmented based on the clustering result. The experiments on artificial images with the noise of different levels and real images demonstrate that the proposed approach can perform segmentation well.

The paper is organized as follows. In Sec. 2, the proposed method is described. The experiments and comparisons are discussed in Sec. 3. Finally, the conclusions are given in Sec. 4.

## 2. Proposed Method

### 2.1. Neutrosophic set

Neutrosophic set and its properties are discussed briefly.<sup>9</sup> Let  $U$  be a universe of discourse, and a neutrosophic set  $A$  is included in  $U$ . An element  $x$  in set  $A$  is denoted as  $x(T, I, F)$ .  $T$ ,  $I$  and  $F$  are real standard or non-standard sets of  $]^{-0}, 1^{+}[$  with  $\sup T = t_{\sup}$ ,  $\inf T = t_{\inf}$ ,  $\sup I = i_{\sup}$ ,  $\inf I = i_{\inf}$ ,  $\sup F = f_{\sup}$ ,  $\inf F = f_{\inf}$  and  $n_{\sup} = t_{\sup} + i_{\sup} + f_{\sup}$ ,  $n_{\inf} = t_{\inf} + i_{\inf} + f_{\inf}$ .  $T$ ,  $I$  and  $F$  are called the neutrosophic components.

An element  $x(T, I, F)$  belongs to  $A$  in the following way: it is  $t\%$  true,  $i\%$  indeterminate, and  $f\%$  false, where  $t$  varies in  $T$ ,  $i$  varies in  $I$ , and  $f$  varies in  $F$ . Statically,  $T$ ,  $I$  and  $F$  are membership sets, but dynamically,  $T$ ,  $I$  and  $F$  are functions/operators depending on known and/or unknown parameters. The sets  $T$ ,  $I$  and  $F$  are not necessarily intervals, and may be any real sub-unitary subsets: discrete or continuous;

single-element, finite, countable or uncountable infinite; union or intersection of various subsets; etc.

**2.2. Neutrosophic image**

Let  $U$  be a universe of the discourse, and  $W \subseteq U$  which is composed by the bright pixels. A neutrosophic image  $P_{NS}$  is characterized by three membership sets  $T$ ,  $I$  and  $F$ .

A pixel  $P$  in the image is described as  $P(t, i, f)$  and belongs to  $W$  in the following way: it is  $t\%$  true,  $i\%$  indeterminate, and  $f\%$  false as a bright pixel, where  $t$  varies in  $T$ ,  $i$  varies in  $I$ , and  $f$  varies in  $F$ .

Pixel  $P(i, j)$  is transformed into the neutrosophic domain.  $P_{NS}(i, j) = \{T(i, j), I(i, j), F(i, j)\}$ .  $T(i, j)$ ,  $I(i, j)$  and  $F(i, j)$  are the membership values belonging to the white set, indeterminate set and non-white set, respectively, which are defined as:

$$T(i, j) = \frac{\bar{g}(i, j) - \bar{g}_{\min}}{\bar{g}_{\max} - \bar{g}_{\min}} \tag{2.1}$$

$$\bar{g}(i, j) = \frac{1}{w \times w} \sum_{m=i-w/2}^{i+w/2} \sum_{n=j-w/2}^{j+w/2} g(m, n) \tag{2.2}$$

$$I(i, j) = \frac{\delta(i, j) - \delta_{\min}}{\delta_{\max} - \delta_{\min}} \tag{2.3}$$

$$\delta(i, j) = \text{abs}(g(i, j) - \bar{g}(i, j)) \tag{2.4}$$

$$F(i, j) = 1 - T(i, j) \tag{2.5}$$

where  $\bar{g}(i, j)$  is the local mean value of the image.  $\delta(i, j)$  is the absolute value of the difference between intensity  $g(i, j)$  and its local mean value  $\bar{g}(i, j)$ .

**2.3.  $\alpha$ -mean operation**

$I(i, j)$  is employed to measure the indeterminacy degree of element  $P_{NS}(i, j)$ . For making  $T$  and  $F$  correlated with  $I$ , the changes in  $T$  and  $F$  should influence the distribution of the elements in  $I$ .

For a gray level image  $Im$ , a mean operation is defined as:

$$\overline{Im}(i, j) = \frac{1}{w \times w} \sum_{m=i-w/2}^{i+w/2} \sum_{n=j-w/2}^{j+w/2} Im(m, n) \tag{2.6}$$

The  $\alpha$ -mean operation for  $P_{NS}$ ,  $\overline{P}_{NS}(\alpha)$ , is defined as:

$$\overline{P}_{NS}(\alpha) = P(\overline{T}(\alpha), \overline{I}(\alpha), \overline{F}(\alpha)) \tag{2.7}$$

$$\bar{T}(\alpha) = \begin{cases} T & I < \alpha \\ \bar{T}_\alpha & I \geq \alpha \end{cases} \quad (2.8)$$

$$\bar{T}_\alpha(i, j) = \frac{1}{w \times w} \sum_{m=i-w/2}^{i+w/2} \sum_{n=j-w/2}^{j+w/2} T(m, n) \quad (2.9)$$

$$\bar{F}(\alpha) = \begin{cases} F & I < \alpha \\ \bar{F} & I \geq \alpha \end{cases} \quad (2.10)$$

$$\bar{F}_\alpha(i, j) = \frac{1}{w \times w} \sum_{m=i-w/2}^{i+w/2} \sum_{n=j-w/2}^{j+w/2} F(m, n) \quad (2.11)$$

$$\bar{I}_\alpha(i, j) = \frac{\bar{\delta}_T(i, j) - \bar{\delta}_{T \min}}{\bar{\delta}_{T \max} - \bar{\delta}_{T \min}} \quad (2.12)$$

$$\bar{\delta}_T(i, j) = \text{abs}(\bar{T}(i, j) - \bar{\bar{T}}(i, j)) \quad (2.13)$$

$$\bar{\bar{T}}(i, j) = \frac{1}{w \times w} \sum_{m=i-w/2}^{i+w/2} \sum_{n=j-w/2}^{j+w/2} \bar{T}(m, n) \quad (2.14)$$

where  $\bar{\delta}_T(i, j)$  is the absolute value of the difference between the mean intensity  $\bar{T}(i, j)$  and its mean value  $\bar{\bar{T}}(i, j)$  after the  $\alpha$ -mean operation.

### 2.4. Image segmentation based on improved fuzzy c-means

Among clustering methods, the fuzzy c-means algorithm is widely used.<sup>13,14</sup> It is important to define an objective function for a clustering analysis method.

#### 2.4.1. Improved fuzzy c-means algorithm

The improved fuzzy c-means algorithm (IFCM) is designed for a neutrosophic image and the membership and convergence criterion are defined.

Considering the effect of indeterminacy, we composed the two sets,  $T$  and  $I$ , into a new value for clustering.

$$X(i, j) = \begin{cases} T(i, j) & I(i, j) \leq \alpha \\ \bar{T}_\alpha(i, j) & I(i, j) > \alpha \end{cases} \quad (2.15)$$

The new partition matrix, objective function and membership are defined for a neutrosophic set as:

$$\tilde{U} = \begin{bmatrix} \mu_{NS1}(1, 1) & \cdots & \mu_{NS} C(1, 1) \\ \cdots & \cdots & \cdots \\ \mu_{NS1}(H, W) & \cdots & \mu_{NS} C(H, W) \end{bmatrix} \quad (2.16)$$

$$J_{NS} = \sum_{l=1}^C \sum_{i=1}^H \sum_{j=1}^W (\mu_{NS \ l}(i, j))^m \|X(i, j) - c_l\|^2 \tag{2.17}$$

$$\mu_{NS \ l}(i, j) = \begin{cases} \frac{1}{\sum_{k=1}^C \sum_{i=1}^H \sum_{j=1}^W \left( \frac{\|T(i, j) - c_l\|}{\|T(i, j) - c_k\|} \right)^{\frac{2}{m-1}}} & I(i, j) \leq \alpha \\ \frac{1}{\sum_{k=1}^C \sum_{i=1}^H \sum_{j=1}^W \left( \frac{\|\bar{T}_\alpha(i, j) - c_l\|}{\|\bar{T}_\alpha(i, j) - c_k\|} \right)^{\frac{2}{m-1}}} & I(i, j) > \alpha \end{cases} \tag{2.18}$$

The mean value of membership matrix  $\bar{U}_{NS}$  is defined in neutrosophic domain as:

$$\bar{U}_{NS} = \sum_{l=1}^C \sum_{i=1}^H \sum_{j=1}^W \mu_{NS \ l}(i, j) \tag{2.19}$$

If the membership remains unchanged, the IFCM is converged and the iterative procedure will be terminated. The entire IFCM is composed of the following steps:

- (1) Initialize the partition matrix  $\bar{U}_{NS}^{(0)}$ ;
- (2) Calculate the center vectors  $C_{NS}^{(k)}$  with  $\bar{U}_{NS}^{(k)}$  at step  $k$ ;

$$c_{NS \ l} = \begin{cases} \frac{\sum_{i=1}^H \sum_{j=1}^W (\mu_{NS \ l}(i, j))^m \cdot T(i, j)}{\sum_{i=1}^H \sum_{j=1}^W (\mu_{NS \ l}(i, j))^m} & I(i, j) \leq \alpha \\ \frac{\sum_{i=1}^H \sum_{j=1}^W (\mu_{NS \ l}(i, j))^m \cdot \bar{T}_\alpha(i, j)}{\sum_{i=1}^H \sum_{j=1}^W (\mu_{NS \ l}(i, j))^m} & I(i, j) > \alpha \end{cases}$$

- (3) Update  $\bar{U}_{NS}^{(k)}$  to  $\bar{U}_{NS}^{(k+1)}$ ;

$$\mu_{NS \ l}^{(k+1)}(i, j) = \begin{cases} \frac{1}{\sum_{k=1}^C \sum_{i=1}^H \sum_{j=1}^W \left( \frac{\|T(i, j) - c_l\|}{\|T(i, j) - c_k\|} \right)^{\frac{2}{m-1}}} & I(i, j) \leq \alpha \\ \frac{1}{\sum_{k=1}^C \sum_{i=1}^H \sum_{j=1}^W \left( \frac{\|\bar{T}_\alpha(i, j) - c_l\|}{\|\bar{T}_\alpha(i, j) - c_k\|} \right)^{\frac{2}{m-1}}} & I(i, j) > \alpha \end{cases}$$

- (4) Compute  $\bar{U}_{NS}^{(k+1)}$  and  $\bar{U}_{NS}^{(k)}$ . If  $|\bar{U}_{NS}^{(k+1)} - \bar{U}_{NS}^{(k)}| < \epsilon$  then stop;

Otherwise return to step (2).

### 2.4.2. Image segmentation based on IFCM

Based on IFCM, a novel image segmentation algorithm is proposed. First, the image is transformed into the neutrosophic domain. Second, the indeterminacy of the neutrosophic set  $P_{NS}$  is decreased using the  $\alpha$ -mean operation on subset  $T$  until the

membership value in IFCM becomes unchanged. Finally, the image is segmented based on the IFCM clustering result.

The entire proposed segmentation method can be described as follows:

- (1) Let the input image be  $Im$ , set  $t = 1$  and  $\overline{Im}^{(t)} = Im$ ;
- (2) Transform  $Im^{(t)}$  into  $NS$  domain  $Im_{NS}^{(t)} = \{T^{(t)}, I^{(t)}, F^{(t)}\}$  at time step  $t$ , and select the value of  $\alpha$  manually;
- (3) Perform the  $\alpha$ -mean operation on the subset  $T^{(t)}$  at time step  $t$ , and obtain the new subset  $T_{\alpha}^{(t)}$ ;
- (4) Apply IFCM to  $T_{\alpha}^{(t)}$ , and compute the new membership matrix  $\underline{U}_{NS}^{(t+1)}$  and its mean value  $\bar{U}_{NS}^{(t+1)}$ ;
- (5) Update the image  $Im_{NS}^{(t+1)} = \{T_{\alpha}^{(t+1)}, I^{(t+1)}, F^{(t+1)}\}$  and  $t = t + 1$ ;
- (6) If  $|\bar{U}_{NS}^{(t+1)} - \bar{U}_{NS}^{(t)}| < \epsilon$ , go to 7); Else go to 2);
- (7) Segment the image according to membership matrix  $\underline{U}_{NS}^{(t)}$ ;

The flowchart of the proposed segmentation algorithm is shown in Fig. 1.

### 3. Experiments and Discussions

We have applied the proposed approach to a variety of images and compared its performance with that of some existing methods.

#### 3.1. Performance evaluation

Reference 15 proposed a modified fuzzy  $c$ -means segmentation algorithm (MFCM),<sup>15</sup> in which fuzzy clustering functions were based on the intensity and average intensity of a pixel neighborhood. It claimed that it had significantly reduced the segmentation error inherent in the traditional fuzzy  $c$ -means approach<sup>5</sup> and Otsu method.<sup>16</sup>

First, we use several synthetic images to compare the performances of the proposed IFCM approach and the MFCM method.<sup>15</sup> Figure 2(a) is an artificial *chess-board* image with two intensities (0 and 255), and Fig. 2(b) is the image added Gaussian noise, whose mean is 0 and standard deviation is 115. Figure 2(c) is the segmentation result using the MFCM method. Figure 2(d) is the result by the proposed method. Many pixels are wrongly segmented in Fig. 2(c), while they are segmented correctly in Fig. 2(d). The regions in Fig. 2(d) are more consistent and homogenous, which are better for further processing.

There is no universally accepted objective criterion to evaluate the performance of the segmentation algorithms yet. However, we know the desired results exactly for the artificial images, and can use some objective criteria to evaluate performance of the algorithms.

To compare the segmentation results of the artificial images, we utilize the metric,<sup>15</sup> and the segmentation error is defined as:

$$e = 1 - \frac{\#(I \cap In)}{\#(I)} \tag{3.1}$$

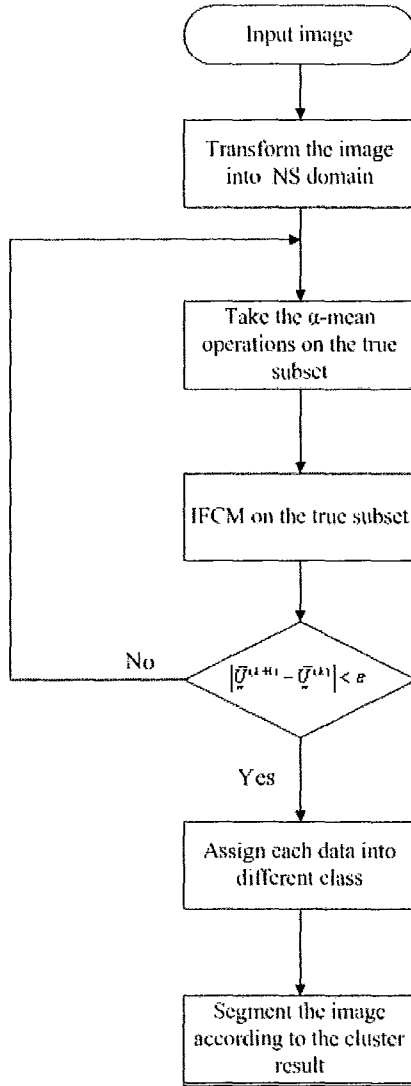


Fig. 1. The flowchart of the segmentation algorithm.

where  $I$  is the ideal segmentation result, and  $I_n$  is the actual segmentation result by the algorithm.  $\#(\cdot)$  is the number of elements in a set.

The segmentation error provides a measure of the misclassified pixels between the ideally segmented image and actually segmented image by the proposed algorithm. The quality of the image can be described in terms of signal-to-noise ratio (SNR):<sup>14</sup>

$$SNR = 10 \log_{10} \left[ \frac{\sum_{r=0}^{H-1} \sum_{c=0}^{W-1} I^2(r, c)}{\sum_{r=0}^{H-1} \sum_{c=0}^{W-1} (I(r, c) - I_n(r, c))^2} \right] \quad (3.2)$$



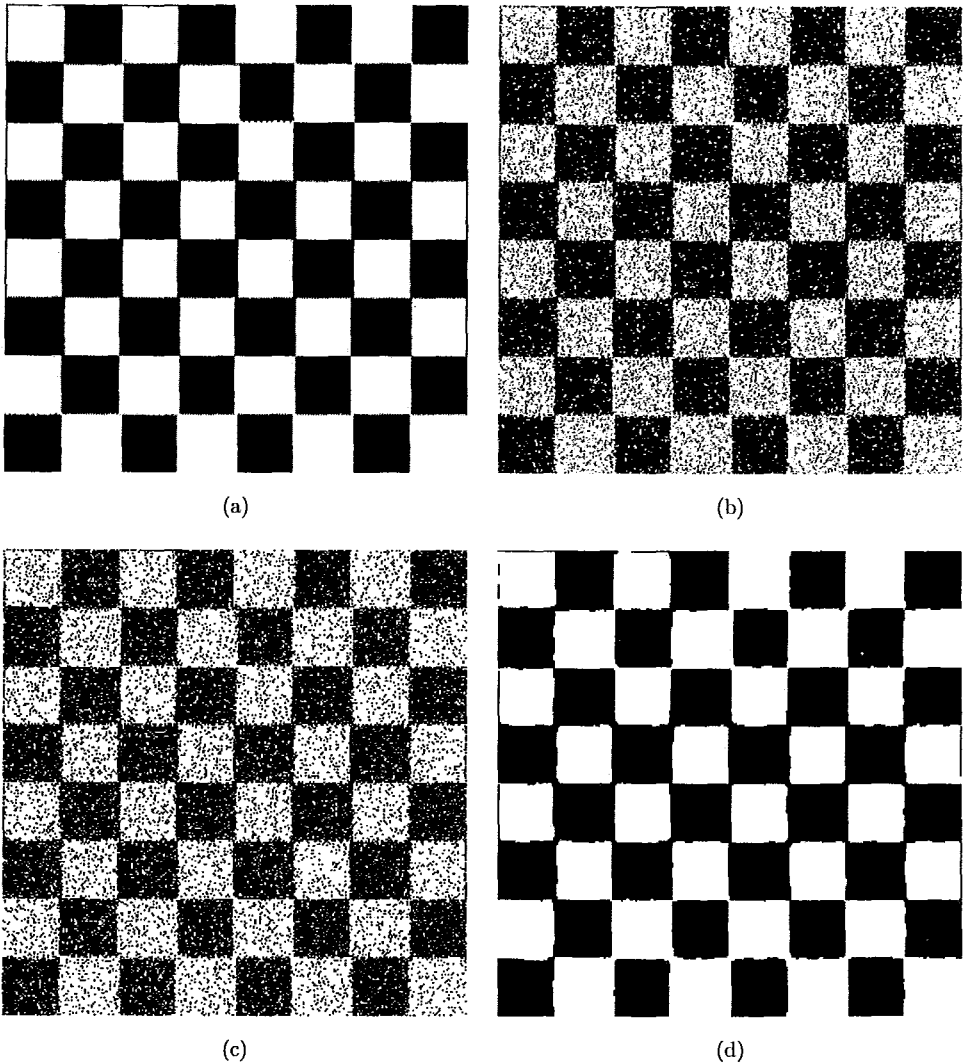


Fig. 2. (a) Original *chessboard* image. (b) Image with Gaussian noise (mean: 0 and standard deviation: 115). (c) Result by MFCM method (d) Result by the proposed method.

where  $I(r, c)$  and  $I_n(r, c)$  represent the intensities of pixel  $(r, c)$  in the ideally segmented and actually segmented images, respectively.

We employ an artificial image *chessboard* with two intensity levels as a noise-free image and the Gaussian noises with different standard deviations are added to the original image to form the new images which are employed to test the MFCM and proposed method. The comparison of the segmentation error and SNR is listed in Table 1. From Table 1, we can see clearly that the proposed method achieves better performance and lower segmentation error at all SNRs. The segmentation errors of the proposed method are all smaller than 0.0119, and the errors of MFCM method are

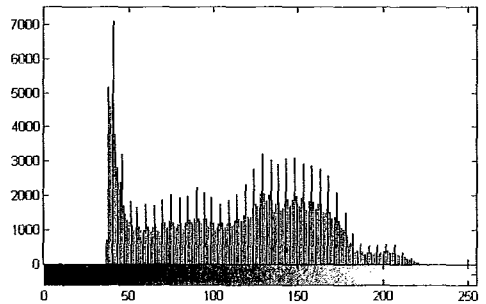
Table 1. The segmentation comparisons of IFCM and MFCM.

Standard deviation	SNR	IFCM	MFCM
20	21.6889	0.0082	0.0081
25	19.8163	0.0077	0.0086
30	18.2624	0.0079	0.0091
35	16.9525	0.0086	0.0096
40	15.8132	0.0087	0.0112
45	14.8045	0.0090	0.0131
50	13.8805	0.0105	0.0169
55	13.0669	0.0099	0.0216
60	12.3097	0.0096	0.0288
65	11.6415	0.0106	0.0376
70	10.9686	0.0095	0.0478
75	10.3932	0.0103	0.0574
80	9.91774	0.0102	0.0675
85	9.33476	0.0106	0.0789
90	8.87745	0.0110	0.0906
95	8.43101	0.0112	0.1012
100	7.99699	0.0124	0.1147
105	7.62658	0.0125	0.1258
110	7.24949	0.0124	0.1352
115	6.97908	0.0119	0.1451
Average	12.3006	0.01010	0.05664

all bigger than that of the proposed method. While the SNR is low, the proposed method performs much better than MFCM. The proposed approach can obtain the optimum segmentation result with error rate 0.0119 which is very low when SNR is 6.9791 dB, while the error of MFCM reaches 0.1451. The average segmentation error



(a)



(b)

Fig. 3. (a) Man image. (b) Histogram of (a). (c) Segmentation result by MFCM. (d) Segmentation result by the proposed method.



(c)



(d)

Fig. 3. (Continued)

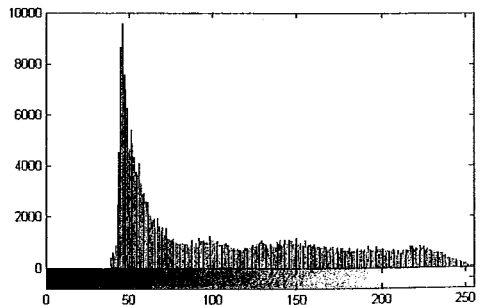
of MFCM is 0.05664, while the average error of IFCM is the 0.01010, i.e. the error rate of MFCM is more than 5 times higher than that of IFCM.

### 3.2. *Experiments on real images*

We have applied the proposed approach to a variety of real images. Due to page limit, only several images are displayed here. Figures 3(a)–6(a) are the original images and



(a)



(b)

Fig. 4. (a) Woman image. (b) Histogram of (a). (c) Segmentation result by MFCM. (d) Segmentation result by the proposed method.



(c)

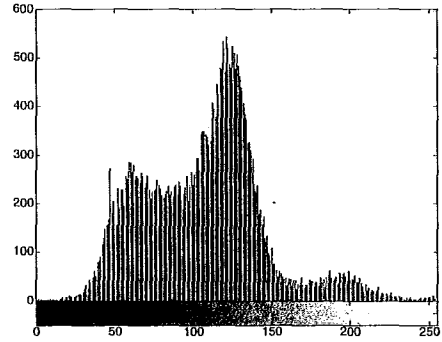


(d)

Fig. 4. (Continued)



(a)



(b)



(c)

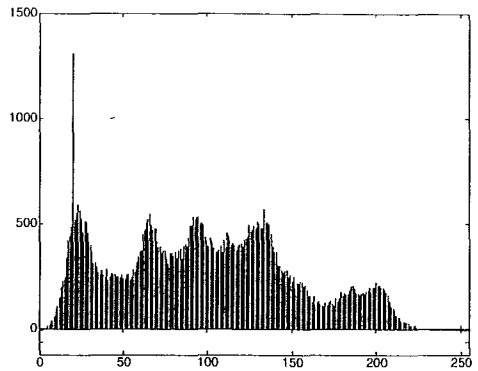


(d)

Fig. 5. (a) Panda image. (b) Histogram of (a). (c) Segmentation result by MFCM. (d) Segmentation result by the proposed method.



(a)



(b)



(c)



(d)

Fig. 6. (a) Lena image. (b) Histogram of (a). (c) Segmentation result by MFCM. (d) Segmentation result of the IFCM method.

Figs. 3(b)–6(b) are the histograms of the original images. Figures 3(c)–6(c) are the results using MFCM method, and Figs. 3(d)–6(d) are the results using the proposed method.

Figure 3(a) is the original image. Figure 3(c) is the segmented image using MFCM algorithm with two classes. The hair regions on his shoulder are not homogenous and over-segmented using the MFCM approach. It is caused by the noise on the hair. However, the IFCM approach can successfully partition the image into the desired regions, as shown in Fig. 3(d), which are more consistent and not affected by noise.

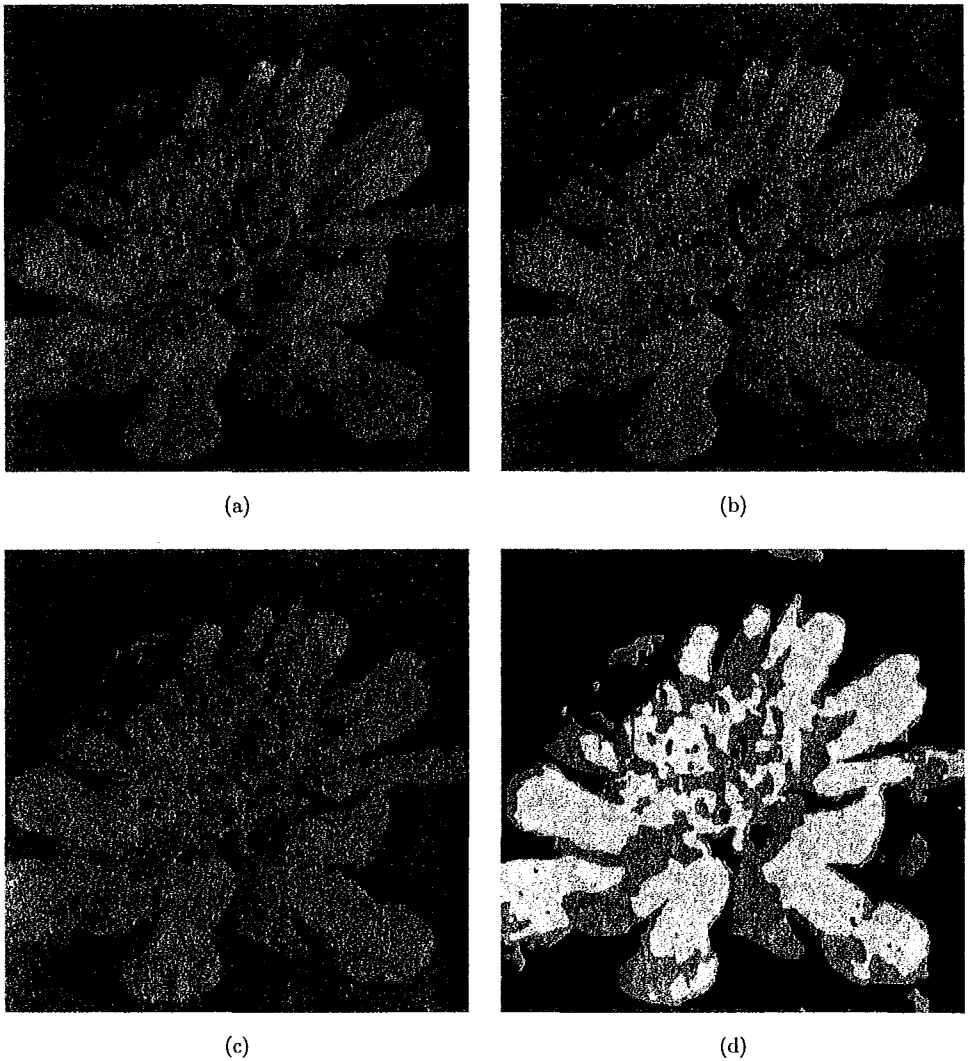


Fig. 7. (a) Flower image. (b) Flower image with Gaussian noise. (c) Result by the MFCM method. (d) Result of the IFCM method.

The man's body has been segmented correctly and the boundaries are smooth and continuous. The man can be extracted from the background completely and correctly.

Figure 4(a) is a woman image whose histogram is shown in Fig. 4(b). The hair regions and neck in Fig. 4(c) are not consistent. The outline of the face is not smooth and distinct. In Fig. 4(d), the hair and neck regions are segmented homogeneously and their boundaries are smooth. In addition, the contour of her face and eyes become distinct and they are easy to be detected.

Figure 5(a) has three main regions: the pandas, stones and grass. Figure 5(b) shows that the image has two significant valleys, which divide the image pixels into



(a)



(b)



(c)



(d)

Fig. 8. (a) Girl image. (b) Girl image with Gaussian noise. (c) Result by the MFCM method. (d) Result of the IFCM method.

three groups. Figure 5(c) is the result of MFCM, which contains some misclassified regions, especially, in the grass and stone regions. In addition, the pandas' backs are affected by some noisy pixels. In Fig. 5(d), the proposed approach makes the three regions distinct and easy to recognize.

Figure 6(a) is the *Lena* image and its histogram is shown in Fig. 6(b). Figure 6(c) is the segmented result using MFCM with three classes. The hair regions and the hat are not homogenous and over segmented in Fig. 6(c). However, the IFCM approach can successfully partition the image into the desired three groups, as shown in Fig. 6(c), which are more consistent and are not affected by noise.

Figure 7(a) is the *Flower* image with low contrast, in which there are three groups: background, petals and the shadows on the petals. In Fig. 7(b), the *Flower* image is corrupted by Gaussian noise, whose mean is 0 and standard deviation is 2.55. The shadows and petals become blurry and they are not distinct. Figure 7(c) is the segmentation result using the MFCM method, which is affected greatly by noise, while the result by the proposed method is much better, as shown in Fig. 7(d).

Figure 8 is another example of noisy image. Figure 8(a) is the *Girl* image and 8(b) is the noisy image with Gaussian noise (mean is 0 and standard deviation is 2.55). The face regions, hat and sweater are corrupted by noise and become not homogeneous. Compared to the segmentation result using the MFCM method in 8(c), the proposed method achieves better segmentation result in Fig. 8(d). The face regions, hat and sweater are segmented correctly, and their edges are distinct and connected smoothly. At the same time, the details, such as the flower on the sweater, are preserved correctly.

In summary, the proposed method not only can segment the clean synthetic images, but also can segment real images with and without noise, since the proposed approach can handle the indeterminacy and uncertainty well.

#### 4. Conclusions

In this paper, a novel segmentation approach is proposed based on neutrosophic theory and modified fuzzy clustering approach. The image is described using three membership sets,  $T$ ,  $F$  and  $I$ . The  $\alpha$ -mean operation is employed iteratively to reduce the indeterminacy. The image becomes more uniform and homogenous after the  $\alpha$ -mean operation, and more suitable for segmentation. The iterative process reaches convergence which is terminated by a measurement. Finally, the image in  $NS$  domain is segmented. The experimental results show that the proposed method cannot only perform better on synthesis images, but also on the real images with/without noise. The proposed approach can find more applications in image processing and pattern recognition.

#### References

1. H. D. Cheng, X. H. Jiang, Y. Sun and J. Wang, Color image segmentation: advances and prospects, *Pattern Recognition* **34**(12) (2001) 2259–2281.
2. J. C. Bezdek, L. O. Hall and L. P. Clarke, Review of MR image segmentation techniques using pattern recognition, *Medical Physics* **20**(4) (1993) 1033–1348.
3. J. K. Udupa and S. Samarasekera, Fuzzy connectedness and object definition: Theory, algorithms, and applications in image segmentation, *Graphical Models and Image Processing* **58**(3) (1996) 246–261.
4. J. C. Dunn, A fuzzy relative of the ISODATA process and its use in detecting compact well-separated clusters, *Journal of Cybernetics* **3**(3) (1973) 32–57.
5. J. C. Bezdek, *Pattern Recognition with Fuzzy Objective Function Algorithms* (Kluwer Academic Publishers Norwell, MA, USA, New York, 1981).



6. D. L. Phan and J. L. Prince, An adaptive fuzzy  $c$ -means algorithm for image segmentation in the presence of intensity inhomogeneities, *Pattern Recognition Letters* **20**(1) (1999) 57–68.
7. L. A. Zadeh, Fuzzy sets, *Inform and Control* **8**(3) (1965) 338–353.
8. H. Wang, R. Sunderraman, F. Smarandache and Y. Q. Zhang, *Interval Neutrosophic Sets and Logic: Theory and Applications in Computing* (Infinite Study, 2005).
9. F. Smarandache, *A Unifying Field in Logics Neutrosophic Logic. Neutrosophy, Neutrosophic Set, Neutrosophic Probability* (American Research Press, 2003).
10. Y. Guo and H. D. Cheng, New neutrosophic approach to image segmentation, *Pattern Recognition* **42**(5) (2009) 587–595.
11. ~~H. D. Cheng and Y. Guo, A new neutrosophic approach to image thresholding, *New Mathematics and Natural Computation* **4**(3) (2008) 291–308.~~
12. Y. Guo and H. D. Cheng, A new neutrosophic approach to image denoising, *New Mathematics and Natural Computation* **5**(3) (2009) 653–662.
13. M. R. Anderberg, *Cluster Analysis for Applications* (1973).
14. R. O. Duda, P. E. Hart and D. G. Stork, *Pattern Classification* (Wiley-Interscience, 2000).
15. L. Ma and R. C. Staunton, A modified fuzzy  $c$ -means image segmentation algorithm for use with uneven illumination patterns, *Pattern Recognition* **40**(11) (2007) 3005–3011.
16. N. Otsu, A threshold selection method from gray-level histograms, *IEEE Transaction on System, Man and Cybernetics* **9**(1) (1979) 62–66.